INTERNATIONAL JOURNAL FOR NUMERICAL METHODS IN FLUIDS
Int. J. Numer. Meth. Fluids 2004; **46**:849–876
Published online 27 September 2004 in Wiley InterScience (www.interscience.wiley.com). DOI: 10.1002/fld.790

Improved non-staggered central NT schemes for balance laws with geometrical source terms

N. Črnjarić-Žic*,†, S. Vuković and L. Sopta

University of Rijeka, Faculty of Engineering, 51000 Rijeka, Vukovarska 58, Croatia

SUMMARY

In this paper we extend the non-staggered version of the central NT (Nessyahu–Tadmor) scheme to the balance laws with geometrical source term. This extension is based on the source term evaluation that includes balancing between the flux gradient and the source term with an additional reformulation that depends on the source term discretization. The main property of the scheme obtained by the proposed reformulation is preservation of the particular set of the steady-state solutions. We verify the improved scheme on two types of balance laws with geometrical source term: the shallow water equations and the non-homogeneous Burger's equation. The presented results show good behaviour of the considered scheme when compared with the analytical or numerical results obtained by using other numerical schemes. Furthermore, comparison with the numerical results obtained by the classical central NT scheme where the source term is simply pointwise evaluated shows that the proposed reformulations are essential. Copyright © 2004 John Wiley & Sons, Ltd.

KEY WORDS: balance laws; central schemes; exact C-property; shallow water equations; non-homogeneous Burger's equation

1. INTRODUCTION

In recent years several numerical schemes have been developed for the numerical treatment of the hyperbolic balance laws. Firstly, one of the most often approaches for solving balance laws was using the fractional step method [1] where first the homogeneous conservation law with some standard numerical scheme for hyperbolic system was solved and then at the next step the source term was incorporated. This technique is quite simple to use, but there are several cases when it is not very effective. The difficulties arise when the source term is stiff or when it is of geometrical type. For that cases, some other, more successful approaches have been developed. There are several papers that consider stiff source terms, for example References [2, 3], in which some classical numerical schemes have been extended to the balance laws such that the source term was evaluated implicitly.

*Correspondence to: N. Črnjarić-Žic, University of Rijeka, Faculty of Engineering, 51000 Rijeka, Vukovarska 58, Croatia.
†E-mail: nelida@riteh.hr

Received 21 August 2003
Revised 19 June 2004

The geometrical source terms arise for example if we consider flow in a channel with bottom topography and/or with varying width or in a nozzle with varying cross-sectional area. These source terms contain a spatial derivative of the geometrical properties of the channel or the nozzle, respectively. The evaluation of the geometrical source term must be done in a quite different way in comparison with the stiff source term evaluation. Namely, it turned out that a successful way for approximating balance law with geometrical source term is to develop the numerical scheme, which is able to capture some steady-state solutions with better accuracy. The mentioned approach was firstly used by Bermùdez and Vázquez in References [4, 5], where they extended the finite volume schemes to the shallow water equations. Moreover, they introduced the notion of the C-property for the schemes that preserve the quiescent flow in the shallow water case exactly. In their work the numerical source term was evaluated such that the upwinding technique was included and additionally the balancing between the flux gradient and the source term was achieved. A similar approach was then used in Reference [6] where the second order finite volume type scheme were extended to the shallow-water equations with an addition of spatially varying flux function. The other type of numerical schemes for the shallow water equations have been developed by LeVeque [7]. His idea was based also on the balancing, but he introduced the modification of the Riemann solver, which results with the scheme that captures quasi-steady states well. Furthermore, in Reference [8] the surface gradient method was used to obtain a numerical scheme with the C-property. The kinetic schemes [9] and the central-upwind schemes [10] have been also developed for the shallow water equations. Recently, in [11] an algebraic technique was presented for balancing flux gradients and source terms when applying Roe's approximate Riemann solver in finite volume schemes.

The goal of our work is to extend the non-staggered central NT scheme to the balance laws with geometrical source term. We consider here two cases: the non-homogeneous Burger's equation and the shallow water equations. The base of this extension lies in preserving some steady-state solutions with the numerical scheme.

In the first section a general formulation of the non-staggered central NT scheme for the balance law is given. In the second section the numerical scheme is completed with the exact definitions for all the terms arising in the numerical scheme, which depend on the particular balance law. First, we consider the non-homogeneous Burger's equation and then the shallow water equations. In order to develop numerical scheme that preserves some steady-state solution, an additional reformulation of the presented scheme is introduced. We refer to this reformulation as to the interface type reformulation, while the finally obtained scheme we call the balanced central NT scheme. The introduced reformulation depends on the discretization of geometrical part of the source term. In the last section the obtained numerical scheme is verified on both considered balance law systems. With the presented test problems we show that numerical results obtained with the balance central NT scheme are very robust and accurate, while on the other hand, the non-balanced version of the scheme produces quite large numerical errors in most of the cases.

2. CENTRAL NT SCHEME FOR BALANCED LAWS

In this section we give a brief overview of the central NT scheme with the extension to the balance laws. More detailed descriptions of the classical central approach can be found in various papers (see for example References [1, 12, 13]).

We consider the one-dimensional balance law system

$$\partial_t u + \partial_x f(u) = g(u,x) \tag{1}$$

with a geometrical type source term $g(u,x)$. According to the staggered mesh used in the numerical scheme development, we introduce two sets of cells: the non-staggered cells $I_i = [x_{i-1/2}, x_{i+1/2}]$, $i = 0,\ldots,N$ and the staggered cells $I_{i+1/2} = [x_i, x_{i+1}]$, $i = 0,\ldots,N-1$. We consider the uniform mesh with a cell size Δx, therefore definitions $x_i = i\Delta x$ and $x_{i+1/2} = x_i + \Delta x/2$ are used. The appropriate notations for the average value of the solution at time $t = t^n$ are used: $\bar{u}_i^n$ denotes the average value of the solution over the non-staggered cell I_i and $\bar{u}_{i+1/2}^n$ is used for the average value over the staggered cell $I_{i+1/2}$. The integration of (1) over the control volume $I_{i+1/2} \times \lfloor t^n, t^{n+1} \rfloor$ yields to

$$\bar{u}_{i+1/2}^{n+1} = \bar{u}_{i+1/2}^n - \frac{1}{\Delta x}\left[\int_{t^n}^{t^{n+1}} f(u(x_{i+1},t))\,\mathrm{d}t - \int_{t^n}^{t^{n+1}} f(u(x_i,t))\,\mathrm{d}t\right] + \frac{1}{\Delta x}\int_{t^n}^{t^{n+1}}\int_{x_i}^{x_{i+1}} g(u(x,t),x)\,\mathrm{d}x\,\mathrm{d}t \tag{2}$$

The terms on the right hand side of (2) have to be numerically approximated. We suppose that the non-staggered values $\bar{u}_i^n$ are known and start with the classical Nessyahu–Tadmor central approach. It is based on the piecewise linear representation of the solution on each grid cell, i.e.

$$u(x,t^n) = \sum_i (\bar{u}_i^n + u_i'(x - x_i))\chi_{I_i}(x) \tag{3}$$

where $\chi_{I_i}(x)$ is the indicator function of interval I_i. The slope u_i' inside the cell is computed by using some slope limiting procedure [1]. A standard choice used also in this paper is minmod limiter

$$u_i' = \mathrm{MM}\left(\frac{u_{i+1} - u_i}{\Delta x}, \frac{u_i - u_{i-1}}{\Delta x}\right) \tag{4}$$

where the minmod function MM is applied to each of the vector component. It is defined by

$$\mathrm{MM}(a,b) = \begin{cases} s\min(|a|,|b|) & \text{if } s = \mathrm{sgn}(a) = \mathrm{sgn}(b) \\ 0 & \text{otherwise} \end{cases} \tag{5}$$

The staggered average $\bar{u}_{i+1/2}^n$ is now evaluated by averaging the piecewise linear representation (3) over the cell $I_{i+1/2}$, i.e.

$$\bar{u}_{i+1/2}^n = \frac{1}{2}(\bar{u}_i^n + \bar{u}_{i+1}^n) + \frac{\Delta x}{8}(u_i' - u_{i+1}') \tag{6}$$

This approximation is second order accurate. To obtain a second order scheme, the integrals in (2) must be evaluated with the same accuracy. First, the flux integral is approximated by

using the one-point Gauss quadrature formula $\int_{t^n}^{t^{n+1}} f(u(x_i,t))\,\mathrm{d}t \approx \Delta x f(u_i^{n+1/2})$. The predictor values $u_i^{n+1/2}$ are evaluated by using relation

$$u_i^{n+1/2} = u_i^n + \frac{\Delta t}{2\Delta x}(-f_i' + g_i^n \Delta x) \tag{7}$$

obtained by the combination of the Taylor expansion and relation (1). Here f_i' approximates the spatial derivative of the flux. As in Reference [12] the quantity f_i' is evaluated by using a slope limiting procedure. More precisely, we apply the relation

$$f_i' = A(\bar{u}_i^n)u_i' \tag{8}$$

and therefore the values u_i' that are already evaluated in (3) can be used. The term g_i^n can be evaluated pointwise or some other approximation can be applied, as we will see in the proceeding of this work.

If the approximation of the source term integral in (2) is defined with $g(u_i^{n+1/2}, u_{i+1}^{n+1/2})\Delta x \Delta t$, the corrector step of the numerical scheme is obtained

$$\bar{u}_{i+1/2}^{n+1} = \bar{u}_{i+1/2}^n - \frac{\Delta t}{\Delta x}(f(u_{i+1}^{n+1/2}) - f(u_i^{n+1/2})) + \Delta t g(u_i^{n+1/2}, u_{i+1}^{n+1/2}) \tag{9}$$

The temporal and the spatial accuracy of order two will be achieved if the definition of the term $g(u_i^{n+1/2}, u_{i+1}^{n+1/2})$ is done appropriately. This term will be defined later, for each considered balance law separately.

We must emphasize that only explicit discretizations of the source term are used in this paper. It is a known fact that the implicit treatment of the source term insures that the numerical scheme becomes more stable. However, this approach is crucial for the cases when the source term is stiff. The nature of the geometrical source term allows us to use the explicit approximations.

Finally, the non-staggered version of the central NT scheme is obtained as described in Reference [12]. To eliminate staggering, the non-staggered average values $\bar{u}_i^{n+1}$ at time t^{n+1} can be obtained by averaging the staggered values following the next procedure. First, the calculated staggered cell averages are used for the construction of a piecewise linear representation

$$\tilde{u}(x,t^{n+1}) = \sum_i (\bar{u}_{i+1/2}^{n+1} + u_{i+1/2}'(x - x_{i+1/2}))\chi_{I_{i+1/2}}(x) \tag{10}$$

Here, the staggered cell derivatives $u_{i+1/2}'$ are computed by applying a slope limiting procedure to the staggered values $\bar{u}_{i+1/2}^{n+1}$. The values $\bar{u}_i^{n+1}$ are then obtained by averaging linear interpolant (10) over the cell I_i, i.e.

$$\begin{aligned}\bar{u}_i^{n+1} &= \frac{1}{\Delta x}\left[\int_{x_{i-1/2}}^{x_i} \tilde{u}(x,t^{n+1})\,\mathrm{d}x + \int_{x_i}^{x_{i+1/2}} \tilde{u}(x,t^{n+1})\,\mathrm{d}x\right] \\ &= \frac{1}{2}(\bar{u}_{i-1/2}^{n+1} + \bar{u}_{i+1/2}^{n+1}) - \frac{\Delta x}{8}(u_{i+1/2}' - u_{i-1/2}')\end{aligned} \tag{11}$$

The complete time step of the non-staggered central NT scheme is illustrated in Figure 1.

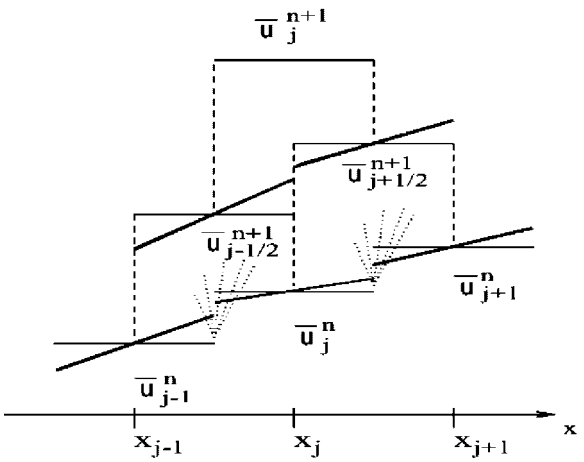

Figure 1. Non-staggered central NT scheme.

We must emphasize that all the computations in the described procedure are defined componentwise and this is the main advantage of the central over the upwind type schemes.

The extension of the central NT scheme to the two-dimensional problems is also possible. The corresponding non-staggered central NT scheme for the homogeneous hyperbolic system is given in Reference [12], while its extension to the two-dimensional balance law could be done in a similar way as it is just described for the one-dimensional case.

3. BALANCED CENTRAL NT SCHEME FOR THE NON-HOMOGENEOUS BURGER'S EQUATION AND FOR THE SHALLOW WATER EQUATIONS

3.1. Non-homogeneous Burger's equation

First, we consider the non-homogeneous Burger's equation with a geometrical source term as defined in Reference [2]

$$\partial_t u + \partial_x \frac{u^2}{2} = -z'(x)u \tag{12}$$

Since the source term depends explicitly on the given function $z(x)$ it is obviously of the geometrical type. For the complete definition of the numerical scheme presented in the previous section it remains to determine the numerical source terms in both, the predictor and the corrector step of the scheme. We define these terms according to the most important property we want to be satisfied by our scheme—the property of preserving steady-state solutions. When we consider the steady-states of system (1), the time evolution is equal zero, so the flux gradient and the source term are in balance. It would be perfect if the balancing could be obtained on numerical level too. For the numerical scheme that is consistent with some steady-state solutions we say it has the exact conservation property. According to the balancing that should be obtained in that case, we refer to the scheme developed in this paper

as to the balanced central NT scheme. For the differential equation (12) the only possible steady-state solution is given with

$$u + z = \text{const} \tag{13}$$

To achieve the mentioned property we evaluate the source term in the predictor step (7) by taking into account the derivative of the variable used in relation (8). More precisely, we propose to take

$$g_i^n = g_{i,L}^n + g_{i,R}^n \tag{14}$$

where

$$g_{i,L}^n = s_i^2 \frac{1 - s_i}{2} g u_i^n \left(-\frac{z_i - z_{i-1}}{\Delta x} \right), \quad g_{i,R}^n = s_i^2 \frac{1 + s_i}{2} g u_i^n \left(-\frac{z_{i+1} - z_i}{\Delta x} \right)$$

and

$$s_i = \begin{cases} -1 & \text{if } u_i' = u_i^n - u_{i-1}^n \\ 1 & \text{if } u_i' = u_{i+1}^n - u_i^n \\ 0 & \text{if } u_i' = 0 \end{cases} \tag{15}$$

The defined parameter s_i depends on the side that is chosen when the variable and the flux derivatives are evaluated. In this way expression (14) includes the source term upwinding and moreover, the obtained source term discretization is in balance with the flux gradient. On the other hand, for the source term in the corrector step (9) we use just a centred discretization, i.e.

$$g(u_i^{n+1/2}, u_{i+1}^{n+1/2}) = \frac{u_i^{n+1/2} + u_{i+1}^{n+1/2}}{2} \left(-\frac{z_{i+1} - z_i}{\Delta x} \right) \tag{16}$$

Let us consider now the steady-state (13). If we include definitions (14) and (16) in (7) and (9), and suppose that the discrete steady-state condition $u_i^n + z_i = \text{const}$ is valid, we can easily see that our numerical scheme reduces to

$$u_i^{n+1/2} = u_i^n \tag{17}$$

and

$$\bar{u}_{i+1/2}^{n+1} = \bar{u}_{i+1/2}^n \tag{18}$$

Hence we can conclude that the time evolution of the variable is equal zero in the steady-state case in the both steps of the defined scheme. For the schemes that do not use the staggered mesh this would be enough to preserve the steady-states. But here some additional reformulations of the procedure of passing from the original to the staggered mesh and vice a versa must be introduced such that the steady-state is preserved. This final step of the considered scheme is presented in Section 3.3.

3.2. Shallow-water equations

Now we apply the non-staggered central NT scheme to the shallow water equations. In the shallow water case the balance law (1) is defined with

$$u=\begin{pmatrix} h \\ hv \end{pmatrix}, \quad f=\begin{pmatrix} hv \\ hv^2+\frac{1}{2}gh^2 \end{pmatrix}, \quad g=\begin{pmatrix} 0 \\ gh(-\frac{\mathrm{d}z}{\mathrm{d}x}) \end{pmatrix} \tag{19}$$

Here $h=h(x,t)$ is the water depth, $v=v(x,t)$ is the water velocity, $z=z(x)$ is the bed level and g is acceleration due to gravity.

As in the Burger's equation, the crucial property we want to be satisfied when the central NT scheme is applied to the shallow water equations is the property of preserving some steady-state solutions. More precisely, we want to preserve the quiescent flow

$$h+z=\text{const}, \quad v=0 \tag{20}$$

By using the terminology given in Reference [4] this is called exact C-property.

We proceed in the similar way as in the Burger's case. Following the idea of decomposing the source term in an upwind manner, we again propose to use the expression

$$g_i^n=g_{i,L}^n+g_{i,R}^n \tag{21}$$

where

$$g_{i,L}^n=s_i^2\,\frac{1-s_i}{2}\begin{pmatrix} 0 \\ -gh_i^n\,\frac{z_i-z_{i-1}}{\Delta x} \end{pmatrix}, \qquad g_{i,R}^n=s_i^2\,\frac{1+s_i}{2}\begin{pmatrix} 0 \\ -gh_i^n\,\frac{z_{i+1}-z_i}{\Delta x} \end{pmatrix}$$

The parameter s_i in the ith cell is here defined with

$$s_i=\begin{cases} -1 & \text{if } h_i'=h_i^n-h_{i-1}^n \\ 1 & \text{if } h_i'=h_{i+1}^n-h_i^n \\ 0 & \text{if } h_i'=0 \end{cases} \tag{22}$$

For the term $g(u_i^{n+1/2},u_{i+1}^{n+1/2})$ we propose to use just the centred approximation

$$g(u_i^{n+1/2},u_{i+1}^{n+1/2})=\begin{pmatrix} 0 \\ g\,\frac{h_i^{n+1/2}+h_{i+1}^{n+1/2}}{2}(-\frac{z_{i+1}-z_i}{\Delta x}) \end{pmatrix} \tag{23}$$

When considering the quiescent flow case, the variable, the flux, and the source term vector reduce to

$$u=\begin{pmatrix} h \\ 0 \end{pmatrix}, \quad f=\begin{pmatrix} 0 \\ \frac{1}{2}gh^2 \end{pmatrix}, \quad g=\begin{pmatrix} 0 \\ gh(-\frac{\mathrm{d}z}{\mathrm{d}x}) \end{pmatrix} \tag{24}$$

With choices (21) and (23) under the quiescent flow condition (20), we can easily see that expressions (7) and (9) reduce to

$$u_i^{n+1/2}=u_i^n \tag{25}$$

and

$$\bar{u}_{i+1/2}^{n+1} = \bar{u}_{i+1/2}^{n} \tag{26}$$

Again, an additional reformulation that preserves the quiescent flow when passing from the non-staggered values to the staggered ones and then back is needed. We present it in the next section.

The part of the source term that concerns friction forces is omitted in (19). It should be added to the second component of the source term in the form $-M^2 v|v|/h^{4/3}$ where $M = M(x)$ denotes Manning's friction factor. However, this term is not geometrical and we evaluate it just pointwise. The other possible approaches and the additional analysis in connection with that term are out of the scope of this paper.

3.3. *The interface type reformulation*

Since the nature of the functions $z(x)$ that appear in the source terms is similar, the reformulation of the scheme will be explained in common for both considered balance laws. The presented reformulation is based on the discretization of the function $z(x)$. Here we suppose the values $z_{i-1/2}$ and $z_{i+1/2}$ on the non-staggered cell boundaries are known for $i = 1, \ldots, N-1$ and then take a linear approximation inside each non-staggered cell, i.e.

$$z(x) = z_i + \frac{z_{i+1/2} - z_{i-1/2}}{\Delta x}(x - x_i) \tag{27}$$

In particular, at the cell centers the relation $z_i = z_{i-1/2} + z_{i+1/2}/2$ is valid.

The reformulation is done as follows. The corrections we propose are connected with the evaluation of u_i' when passing to the staggered mesh and with the evaluation of the term $u_{i+1/2}'$ that appears in the procedure of returning to the non-staggered mesh.

Notice first that when the quiescent flow in the shallow water case is considered, the second component of the variable vector is equal zero, so the modifications are needed just for the first component, i.e. for the variable h. Therefore, the purpose of our reformulation is to preserve the variable u in the Burger's case and the variable h in the shallow-water case. We denote these variables with w, i.e. $w = u$ in the first case and $w = h$ in the second case. The values that are constant at the considered steady-states in both the cases are then equal $w + z$, so we define

$$W = w + z$$

When the central NT scheme is used, the variable w and the function z are supposed to be linear inside each cell. We propose to determine the linearization of the variable w indirectly by prescribing first a linearization of the value $W(x)$ and then by using a relation

$$w(x) = W(x) - z(x)$$

The linearization $W(x)$ inside a cell I_i is obtained by applying a slope limiting procedure on the cell values W_i. Thus, for $x \in I_i$ we have

$$W(x) = W_i + W_i'(x - x_i) \tag{28}$$

The derivation of the original variable can be obviously calculated as

$$w_i' = W_i' - \frac{z_{i+1/2} - z_{i-1/2}}{\Delta x} \tag{29}$$

To obtain the derivations over the staggered mesh the following procedure is proposed. Because function z is not linear inside the non-staggered cell, the values $W_{i+1/2}$ are not constant over the numerical domain. Instead we define the point values that should be used for the linear approximation over the staggered mesh with

$$\tilde{W}_{i+1/2} = w_{i+1/2} + \tilde{z}_{i+1/2} \tag{30}$$

Here the term $\tilde{z}_{i+1/2} = z_{i+1/2} - \frac{1}{2}(z_{i+1/2} - (z_i + z_{i+1})/2)$ is a corrected z value that arises because of nonlinearity over the staggered cell $I_{i+1/2}$. Now the discrete derivatives $\tilde{W}'_{i+1/2}$ are derived using the standard slope limiting procedure and the staggered values $\{\tilde{W}_{i+1/2}\}$. Finally, the relation

$$w'_{i+1/2} = \tilde{W}'_{i+1/2} - \frac{z_{i+1} - z_i}{\Delta x} \tag{31}$$

is applied.

With the described procedures for determining the corresponding linearizations over the cells, the improved non-staggered central NT scheme is consistent with all steady-state solutions for the non-homogeneous Burger's case and with the quiescent flow in the shallow-water case. That is proved in the following way.

From relation (26) follows that the staggered values do not change in the time step of the numerical scheme. Therefore it is enough to prove that the procedure of passing to the staggered values and then back to the non-staggered ones return us the same values we start from. We concentrate just on the variable w that covers both cases.

The steady-state condition at the discrete level is equal

$$W_i = \bar{w}_i + z_i = \text{const} \tag{32}$$

First, for the staggered values that are obtained from the non-staggered ones by examining relations (6) and (29) we get

$$\begin{aligned}
\bar{w}^n_{i+1/2} &= \frac{1}{2}(\bar{w}^n_i + \bar{w}^n_{i+1}) + \frac{\Delta x}{8}(w'_i - w'_{i+1}) \\
&= \frac{1}{2}(\bar{w}^n_i + \bar{w}^n_{i+1}) + \frac{1}{8}(W'_i \Delta x - (z_{i+1/2} - z_{i-1/2}) - W'_{i+1}\Delta x + (z_{i+3/2} - z_{i+1/2})) \\
&= \frac{1}{2}(\bar{w}^n_i + \bar{w}^n_{i+1}) - \frac{1}{2}\left(z_{i+1/2} - \frac{z_i + z_{i+1}}{2}\right)
\end{aligned} \tag{33}$$

The last equality follows from the fact that $W_i' = W'_{i+1} = 0$ at the considered steady-state and additionally by applying the relations $z_{i+1/2} - z_{i-1/2} = 2(z_{i+1/2} - z_i)$ and $z_{i+3/2} - z_{i+1/2} = 2(z_{i+1} - z_{i+1/2})$.

Since relations (18) and (26) are valid, the inclusion of (33) in (30) gives us

$$\tilde{W}_{i+1/2}^{n+1} = \frac{\bar{w}_i^n + \bar{w}_{i+1}^n}{2} + \frac{z_i + z_{i+1}}{2}$$

Because of (32), the values $\tilde{W}_{i+1/2}^{n+1}$ are equal over the whole numerical domain.

Finally, the non-staggered values are evaluated from (11) by using (31)

$$\begin{aligned}\bar{w}_i^{n+1} &= \frac{1}{2}(\bar{w}_{i-1/2}^{n+1} + \bar{w}_{i+1/2}^{n+1}) - \frac{\Delta x}{8}(w'_{i+1/2} - w'_{i-1/2}) \\ &= \frac{1}{2}(\bar{w}_{i-1/2}^{n+1} + \bar{w}_{i+1/2}^{n+1}) - \frac{1}{8}(\tilde{W}'_{i+1/2}\Delta x - (z_{i+1} - z_i) - \tilde{W}'_{i-1/2}\Delta x + (z_i - z_{i-1}))\end{aligned} \quad (34)$$

By including (33) in the above expression and by using the fact $\tilde{W}'_{i-1/2} = \tilde{W}'_{i+1/2} = 0$ we obtain

$$\bar{w}_i^{n+1} = \bar{w}_i^n$$

With this we finish the proof of the consistency with the steady-state cases, so the balanced central NT scheme is constructed.

4. NUMERICAL RESULTS

In this section we present numerical results obtained with the improved non-staggered central NT scheme on several test problems for the non-homogeneous Burger's equation and for the shallow water equations.

4.1. Non-homogeneous Burger's equation

This test problem was suggested by Jin [2]. The Burger's equation (12) is considered on the domain $[0, 10]$ with the initial condition $u(x, 0) = 0,\ x > 0$ and the boundary condition $u(0, t) = 2,\ t > 0$. Here we test the ability of preserving steady-state for the case of the scalar balance law in both: continuous and discontinuous $z = z(x)$ function case. The steady-state analytical solution for the given problem is equal

$$u = 2 - z \quad (35)$$

In the continuous case $z(x)$ is given by

$$z(x) = \begin{cases} \cos(\pi x) & \text{if } 4.5 \leqslant x \leqslant 5.5 \\ 0 & \text{otherwise} \end{cases} \quad (36)$$

while in the discontinuous one

$$z(x) = \begin{cases} \cos(\pi x) & \text{if } 5 \leqslant x \leqslant 6 \\ 0 & \text{otherwise} \end{cases} \quad (37)$$

In Figures 2 and 3 we present results for both cases. We compare with the exact solution the numerical results obtained with the balanced central NT scheme and with the standard

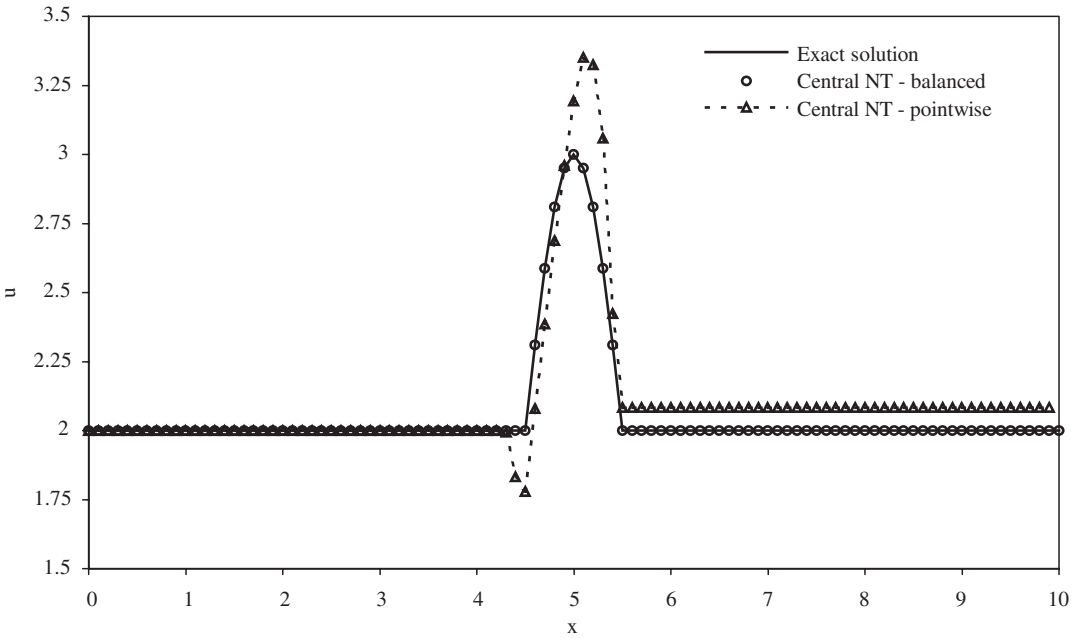

Figure 2. Comparison of the solutions in the continuous case, Section 4.1.

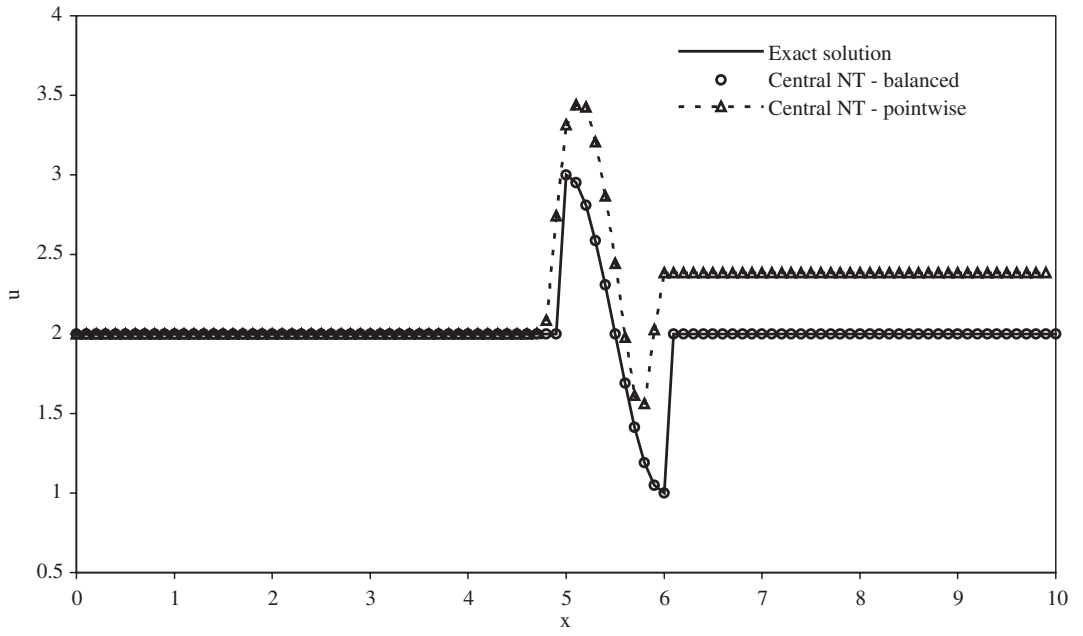

Figure 3. Comparison of the solutions in the discontinuous case, Section 4.1.

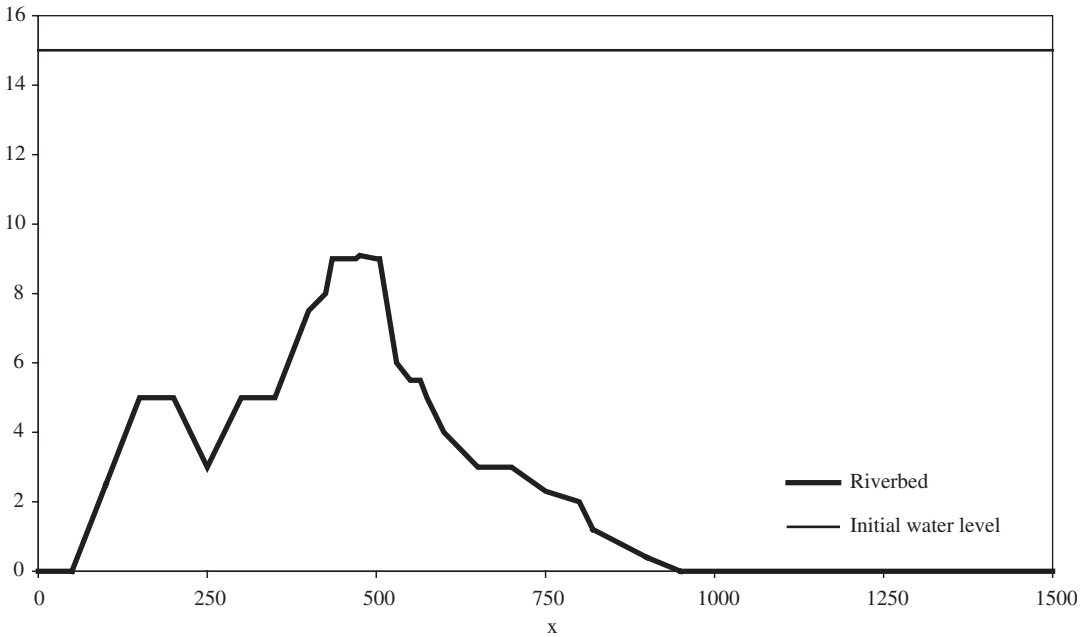

Figure 4. Initial water level for the quiescent flow test case, Section 4.2.1.

central NT scheme where no reformulations are included and the source term is just pointwise evaluated. The space step is set to $\Delta x = 0.1$. The exact solution and the numerical one obtained with the balanced central NT scheme coincide very well. That was what we expect since the balanced central NT scheme is developed in order to preserve steady-states. On the other hand the pointwise version of the central NT scheme produces large numerical errors in both cases.

4.2. Shallow-water equations

4.2.1. A quiescent flow test proposed by the Working Group of Dam Break Modelling. Now, we are interested in the quiescent steady state preserving property of our scheme. The riverbed geometry in this test case is extremely rough, defined as proposed by the Working Group of Dam Break Modelling [4]. The water level is initially defined with $H = 15$ m and water is supposed to be at rest. The riverbed and the initial water level are presented in Figure 4. In Figures 5 and 6 we can see the improvement of the balanced central NT scheme over the non-balanced one. The numerical errors that appear when just the pointwise source term evaluation is used are unacceptably large.

4.2.2. A convergency test over the bed with two bumps. In order to check the accuracy properties of the developed numerical scheme, we apply it on the steady state problem with a given constant discharge and a continuous riverbed. Since in the homogeneous case the balanced central NT scheme is second order accurate, we expect this order is not deteriorated with the reformulations introduced in this work for the considered balance law.

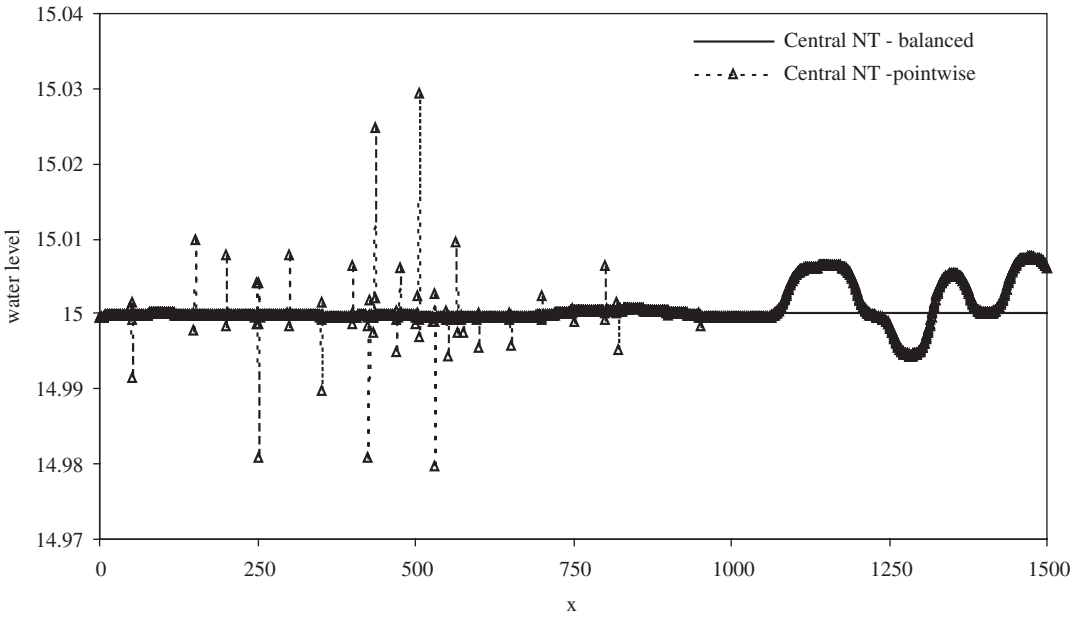

Figure 5. Comparison in water level for the quiescent flow test case at $t = 100$ s, Section 4.2.1.

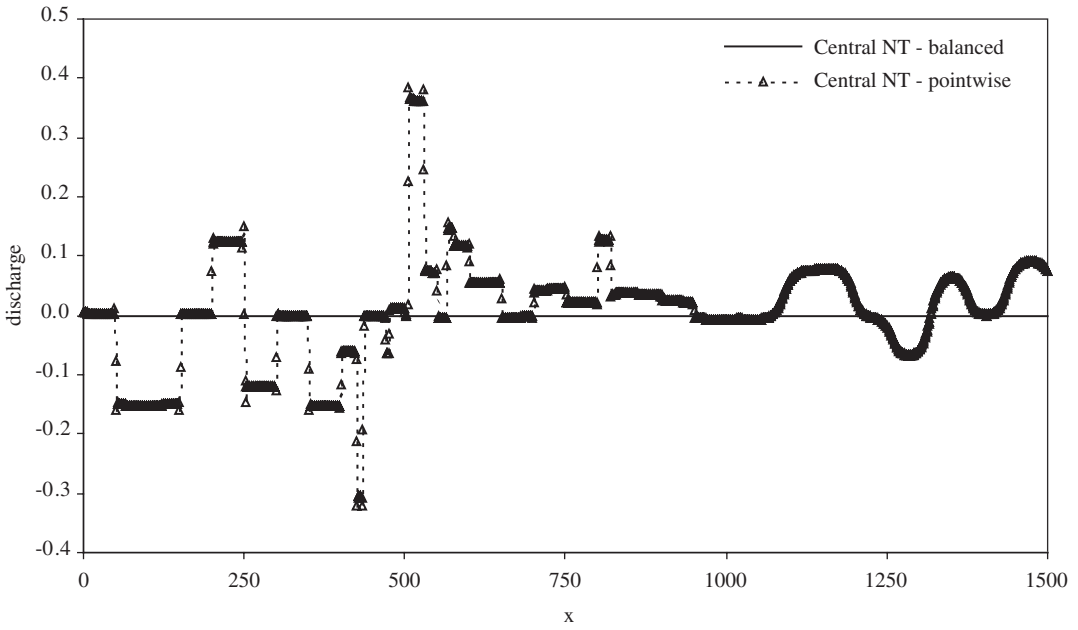

Figure 6. Comparison in discharge for the quiescent flow test case at $t = 100$ s, Section 4.2.1.

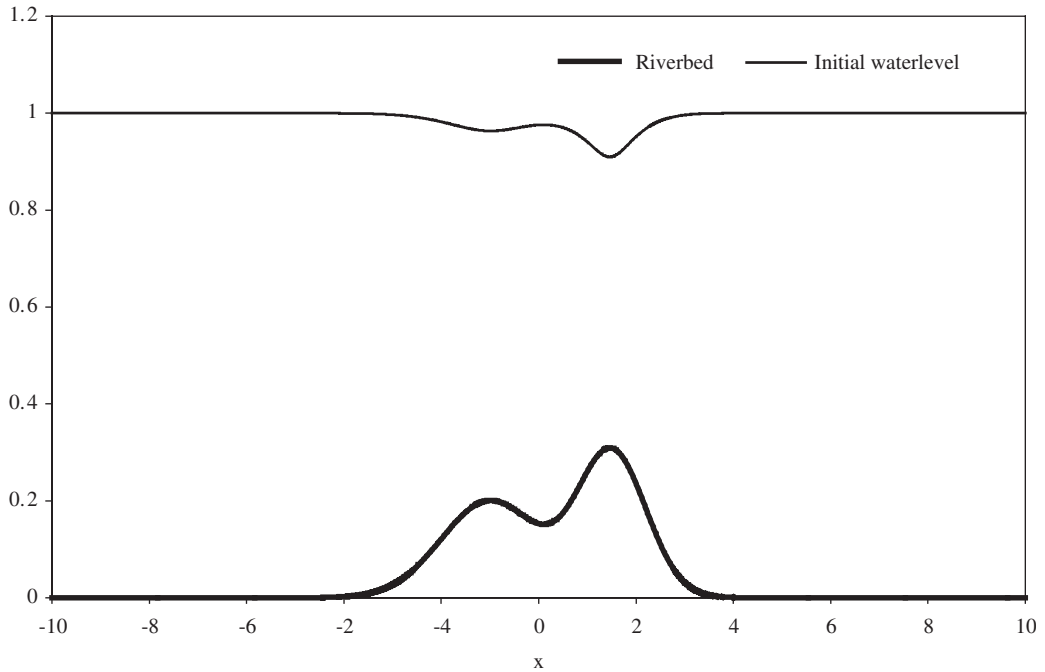

Figure 7. Initial water level for the test problem in Section 4.2.2.

The riverbed is here defined with

$$z(x) = 0.2\exp[-\tfrac{1}{2}(x+1)^2] + 0.3\exp[-(x-1.5)^2] \tag{38}$$

over the domain $[-10, 10]$. The left boundary condition is defined with the discharge $Q(-10, t) = 1\ \mathrm{m}^2/\mathrm{s}$, while on the right boundary the constant water depth $h(10, t) = 1\ \mathrm{m}$ is imposed. The initial water level can be evaluated analytically as a stationary solution with the given constant discharge. This analytical solution is presented in Figure 7 and it should be preserved when numerical scheme is applied. In Figure 8 we can see that as a mesh is refined the numerical solution converges to the exact one.

Furthermore, in Table I we give the convergency test results. Since the numerical scheme attains the order of accuracy equal 2, we can conclude that the improved scheme order is not deteriorated with the reformulation proposed in this work. The CFL coefficient used in all the computations is $c_{\mathrm{cfl}} = 0.5$.

4.2.3. Tidal wave propagation in a relatively short channel with a continuous bottom. We consider now an unsteady test problem proposed by Bermùdez and Vázquez [4]. It is used to establish the correctness of the central NT scheme in the case of a gradually varied flows. The tidal wave propagation occurs in the channel with the length $L = 14\,000\ \mathrm{m}$ and with the

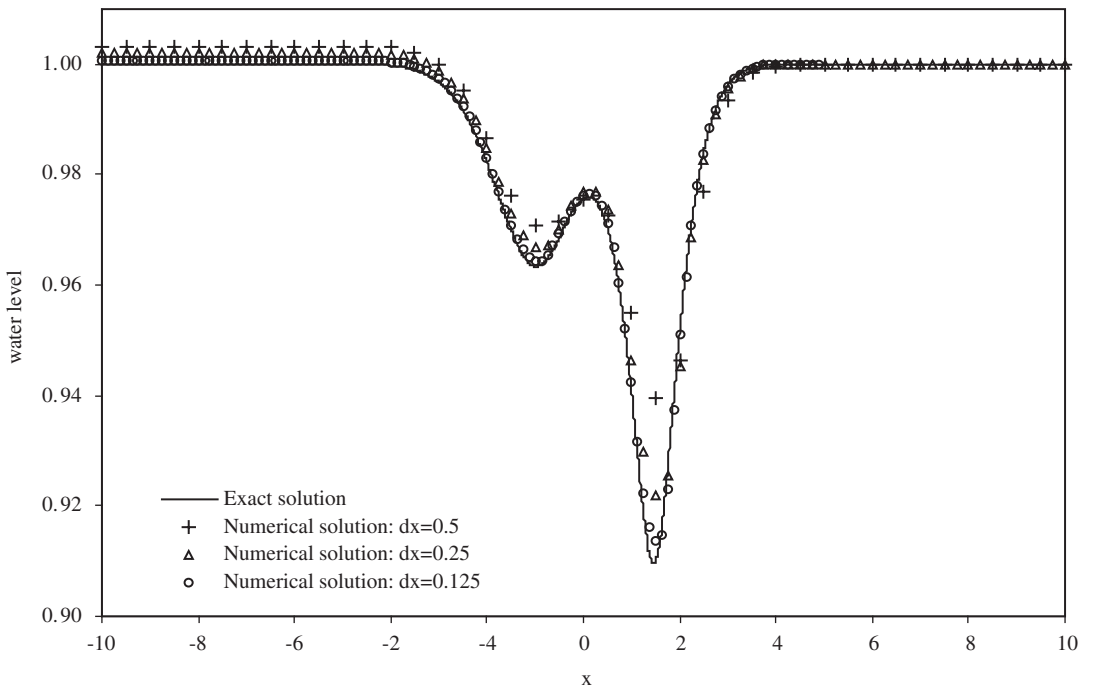

Figure 8. Comparison in water level for different mesh sizes, Section 4.2.2.

Table I. Accuracy of the central NT scheme, Section 4.2.2.

N	L_1 error	L_1 order	L_∞ error	L_∞ order
Errors in water level				
80	1.78×10^{-3}		1.21×10^{-2}	
160	5.63×10^{-4}	1.66	4.77×10^{-3}	1.34
320	1.32×10^{-4}	2.09	1.55×10^{-3}	1.62
40	3.02×10^{-5}	2.13	4.65×10^{-4}	1.74
1280	7.63×10^{-6}	1.98	1.17×10^{-4}	1.98
Errors in discharge				
80	9.62×10^{-4}		1.08×10^{-2}	
160	2.93×10^{-4}	1.72	5.17×10^{-3}	1.06
320	7.39×10^{-5}	1.99	1.75×10^{-3}	1.56
640	1.80×10^{-5}	2.04	5.01×10^{-4}	1.81
1280	4.45×10^{-6}	2.01	1.25×10^{-4}	2.00

riverbed bottom

$$z(x) = 10 + \frac{4x}{L} + 10\sin\left[\pi\left(\frac{4x}{L} - \frac{1}{2}\right)\right] \tag{39}$$

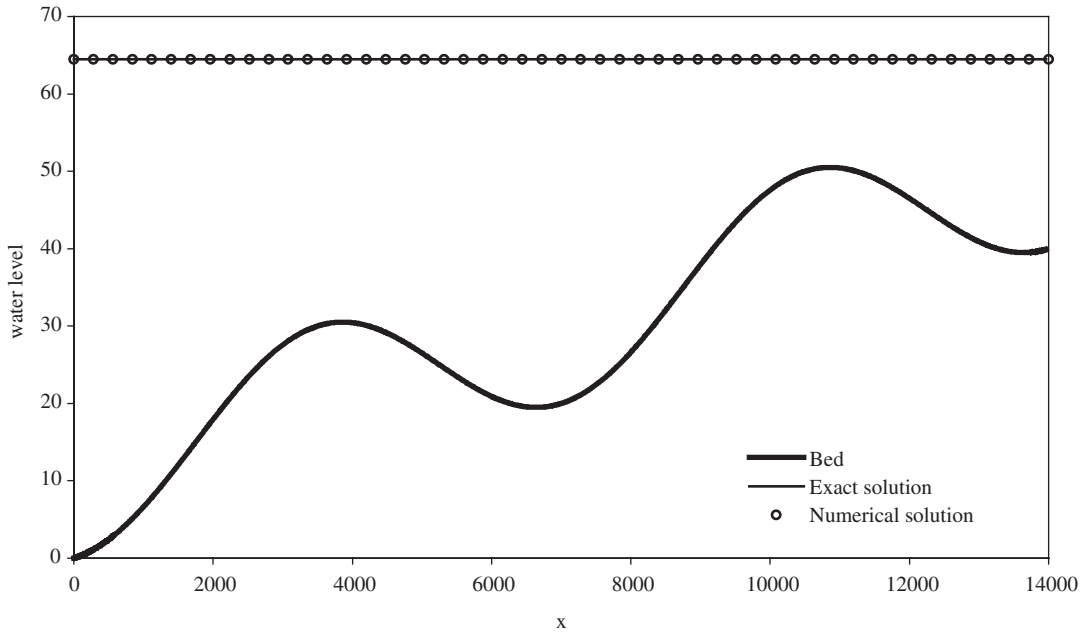

Figure 9. Water level after $t = 10\,800$ s of tidal wave propagation, Section 4.2.3.

The water is initially at rest with constant water level $H(x) = 60.5$ m. The boundary conditions are defined with

$$h(0,t) = H(x) + 4.0 - 4.0 \sin\left[\pi\left(\frac{4t}{86\,400} + \frac{1}{2}\right)\right] \tag{40}$$

and

$$v(L,t) = 0 \tag{41}$$

Equation (40) simulates a tidal wave of 4 m amplitude. Using the asymptotic analysis based on the small Froude numbers (see Reference [4]), an approximate solution is obtained

$$h(x,t) = 64.5 - z(x) - 4.0 \sin\left[\pi\left(\frac{4t}{86\,400} + \frac{1}{2}\right)\right] \tag{42}$$

and

$$v(x,t) = \frac{(x-L)\pi}{5400h(x,t)} \cos\left[\pi\left(\frac{4t}{86\,400} + \frac{1}{2}\right)\right] \tag{43}$$

In Figure 9 we present results in water level obtained by using a relatively coarse grid with space step $\Delta x = 280$ m at time $t = 10\,800$ s. The agreement of the asymptotic and numerical solutions is great. Furthermore, the comparison of the velocity profiles obtained by two different mesh sizes with the asymptotic one is presented in Figure 10. One can note that the numerical results are satisfying and obviously converge to the exact solution.

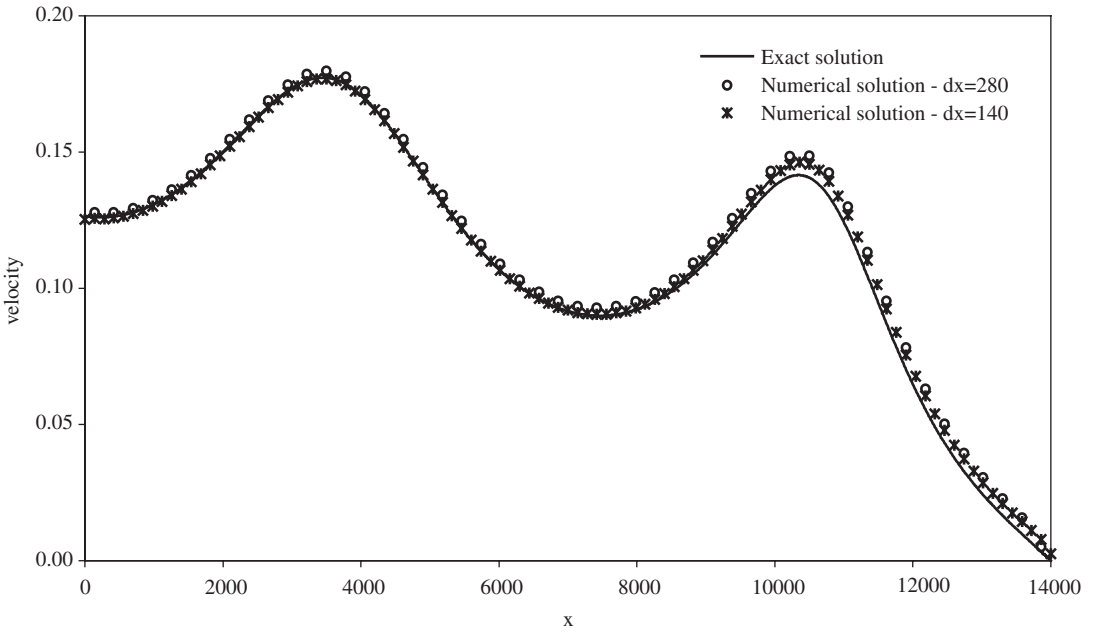

Figure 10. Comparison of the velocity profiles with different mesh sizes with the asymptotic solution after $t = 10\,800$ s of tidal wave propagation, Section 4.2.3.

4.2.4. Tidal wave over a rectangular bump. The purpose of this numerical example is to test the presented numerical scheme for an unsteady problem in the case when discontinuity in the riverbed appears. The considered problem is taken from [14]. The riverbed is given with

$$z(x) = \begin{cases} 8 & \text{if } |x - 1500/2| < 1500/8 \\ 0 & \text{otherwise} \end{cases} \tag{44}$$

while initially the water level is supposed to be constant and equal 16 m. This initial water level is presented in Figure 11. The tidal wave incoming from the left boundary, defined as in the previous example with (40), remedies the initially still water. On the right boundary the water velocity is set to zero just as the Manning friction factor over the complete numerical domain. The computations are performed with the space step $\Delta x = 7.5$ m and $c_{\text{cfl}} = 0.5$. We give the numerical results after $t = 10\,800$ s. In Figure 12 we compare first the balanced and pointwise central NT scheme. The water level after half-time of the tidal wave period passes should be equal 20 m and that is exactly obtained with the balanced central NT scheme. The errors again arise when the pointwise scheme is used. Thus, the superiority of the improved scheme is illustrated again.

In order to test the ability of the central NT schemes to achieve proper shape and speed of a disturbance, we compare the balanced central NT scheme results with an asymptotic solution evaluated following expression (43), which is valid for this test problem also. The numerically obtained velocity profile at $t = 10\,800$ s is compared with the asymptotic one in

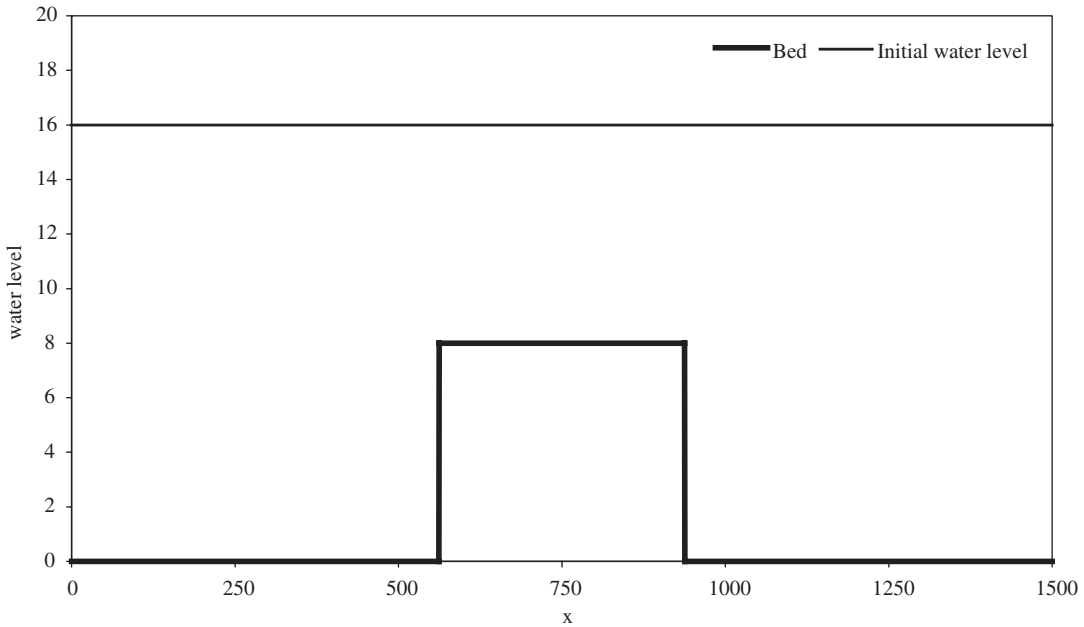

Figure 11. Initial water level for tidal wave over a rectangular bump, Section 4.2.4.

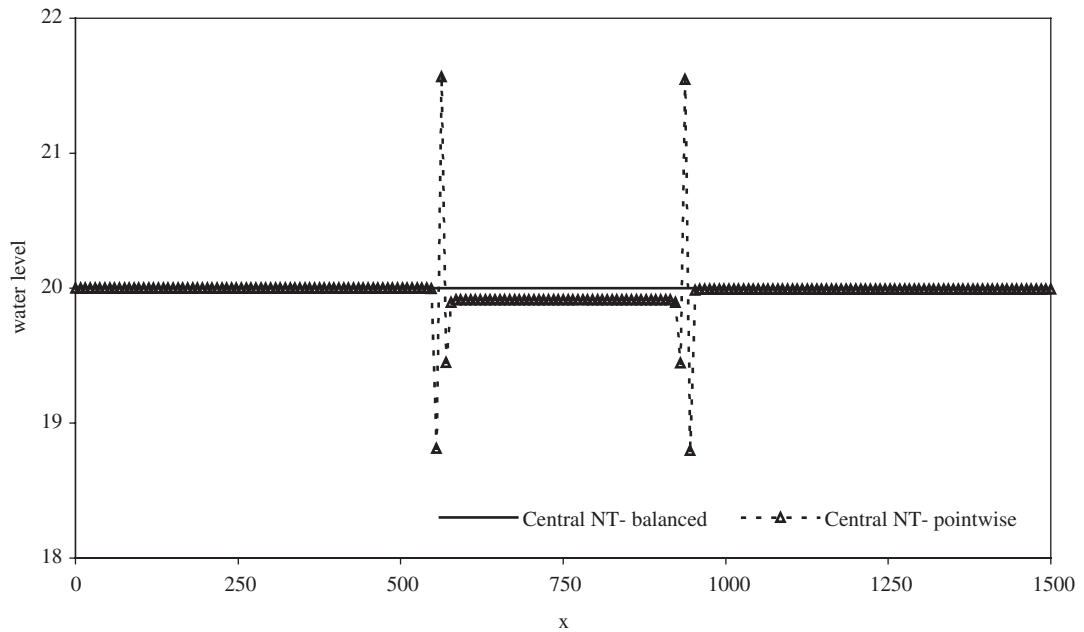

Figure 12. Comparison in water level after $t = 10\,800$ s of tidal wave propagation, Section 4.2.4.

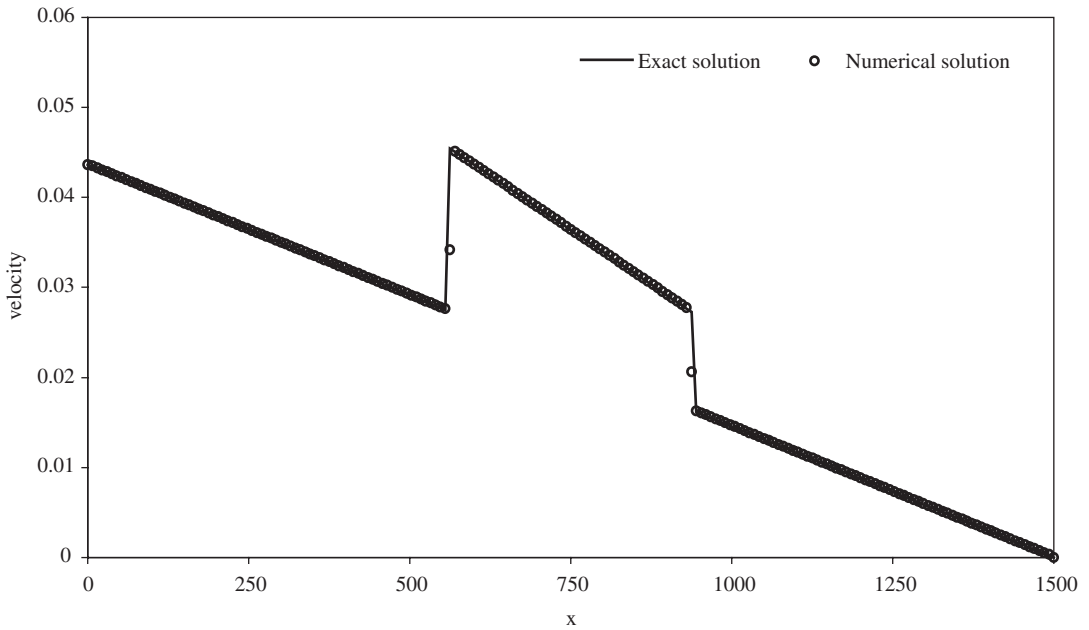

Figure 13. Comparison with an asymptotic solution. Velocity after $t = 10\,800$ s of tidal wave propagation, Section 4.2.4.

Figure 13. The agreement is great. This suggest that the proposed scheme is accurate for tidal flow over an irregular bed.

4.2.5. Dam break problem over a continuous riverbed. This is an initial test problem proposed in Reference [2]. We observe here the behaviour of both, balanced and pointwise version of the central NT scheme on the test problem with discontinuous initial data and continuous riverbed. The riverbed is given with

$$z(x) = 1.398 - 0.347 \tanh(8x - 4) \tag{45}$$

while the initial conditions are

$$h(x,0) = \begin{cases} 1.0 & \text{if } x \leqslant 0.6 \\ 0.2 & \text{if } x > 0.6 \end{cases} \quad \text{and} \quad v(x,0) = 0 \tag{46}$$

We consider here the spatial domain $[0,1]$. In Figure 14 we present the initial water level. As in the original test problem, the gravitational constant is set to $g = 1$. The computations are performed with the space step $\Delta x = 0.01$ m and by using $c_{\text{cfl}} = 0.5$. The behaviour of the solution is similar as in the classical dam-break problem: the rarefaction that arises propagates to the left, while on the right hand side of the initial discontinuity a shock propagating to the right occurs. The 'exact' solution is computed by using balanced flux limited second order finite volume scheme [6] on a very fine grid with the space step $\Delta x = 0.0005$. The comparison with the numerical solution obtained by using the balanced central NT scheme on a much

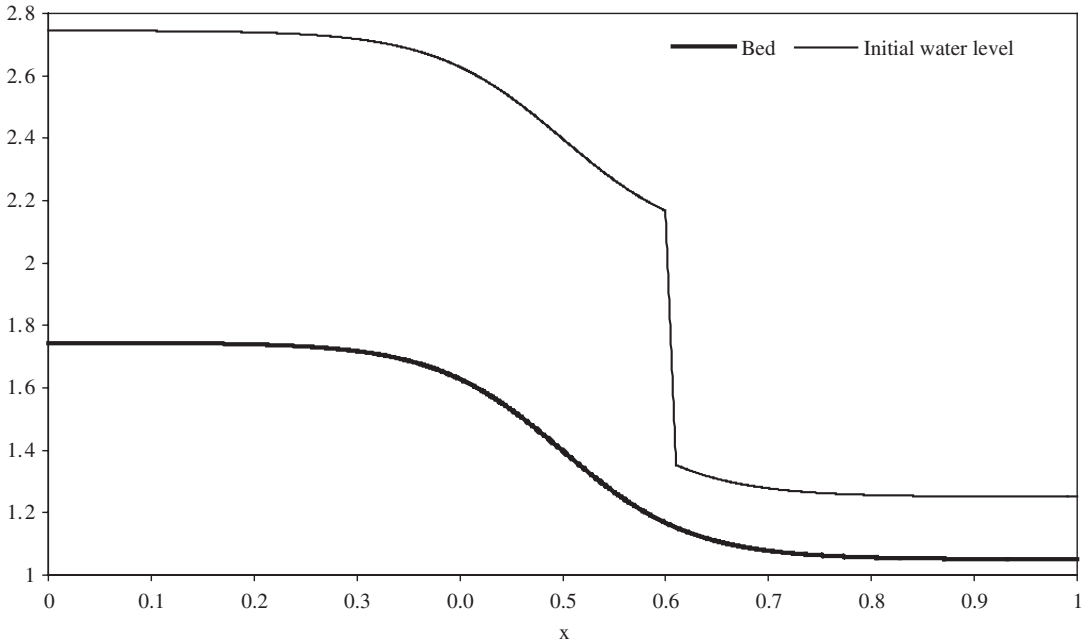

Figure 14. Initial water level for the dam break problem over a continuous riverbed, Section 4.2.5.

coarser grid with $\Delta x = 0.01$ is then made in Figure 15. Moreover, in Figure 16 we show once again that the reformulation introduced in the paper is essential. Namely, the results obtained with the pointwise central NT scheme are completely inaccurate.

4.2.6. LeVeque test example over bump. With this test we check the correctness of the wave speed propagation of the developed numerical scheme when a small disturbance in the water level arises. The test problem is suggested by LeVeque [7]. The bottom topography is defined with

$$z(x) = \begin{cases} 0.25(\cos(10\pi(x-0.5))+1) & \text{if } |x-0.5| < 0.1 \\ 0 & \text{otherwise} \end{cases} \tag{47}$$

over the domain $[0,1]$. The initial conditions are defined with

$$v(x,0) = 0 \quad \text{and} \quad h(x,0) = \begin{cases} 1.0 - z(x) + \varepsilon & \text{if } 0.1 < x < 0.2 \\ 1.0 - z(x) & \text{otherwise} \end{cases} \tag{48}$$

The two cases are considered: $\varepsilon = 0.2$ and 0.01. The initial conditions for the first test case are presented in Figure 17. As in Reference [7] we take $g = 1$. A small perturbation that is defined with the initial condition splits into two waves. The first wave propagates to the left while the right one moves over the bump. The flow in this test case is the quasi-steady state flow. The results are shown at time $t = 0.7$ s. We take a space step $\Delta x = 0.005$. The disturbance caused by the varying riverbed bottom can be clearly seen in Figures 18 and 19. The 'exact' solution

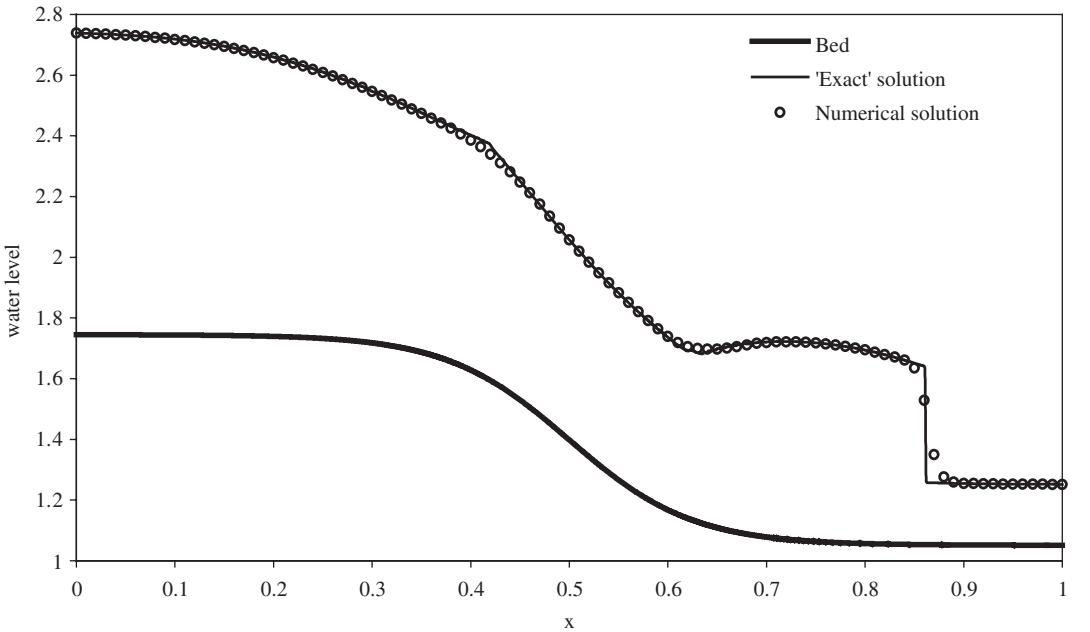

Figure 15. Comparison of the balanced central NT scheme with the 'exact' solution in the dam-break problem. Water level at $t = 0.25$ s, Section 4.2.5.

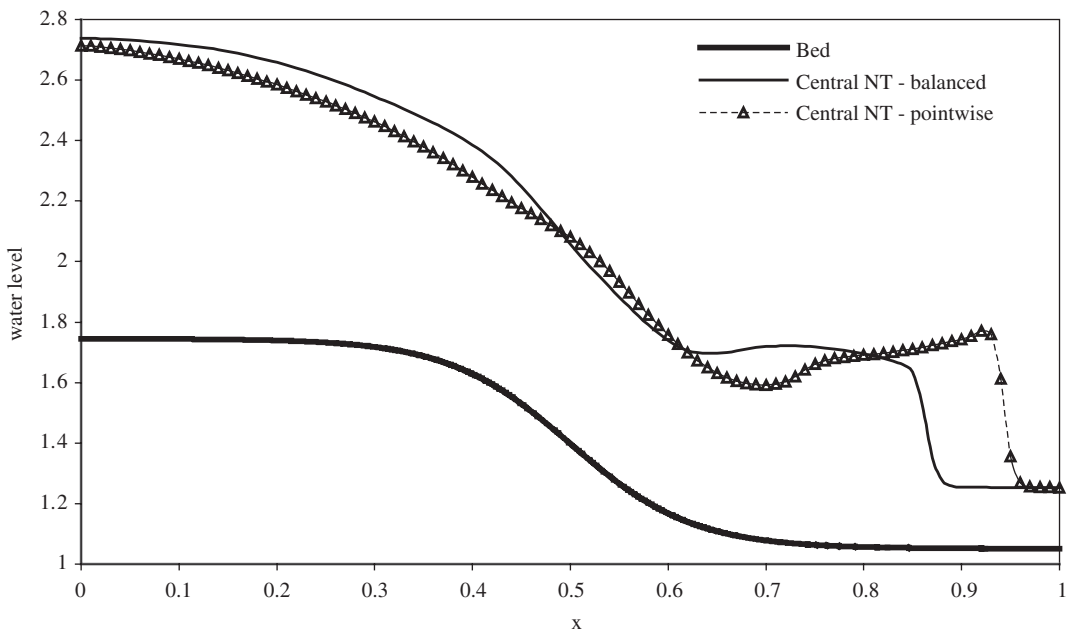

Figure 16. Water level at $t = 0.25$ s for the dam-break problem, Section 4.2.5.

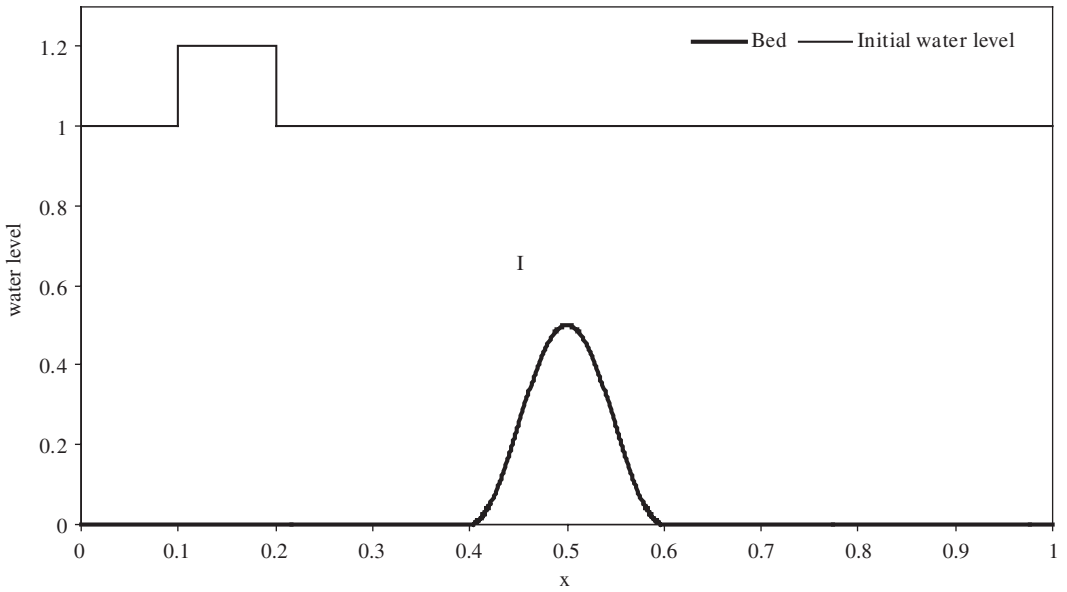

Figure 17. Initial water level for the LeVeque test example with $\varepsilon = 0.2$, Section 4.2.6.

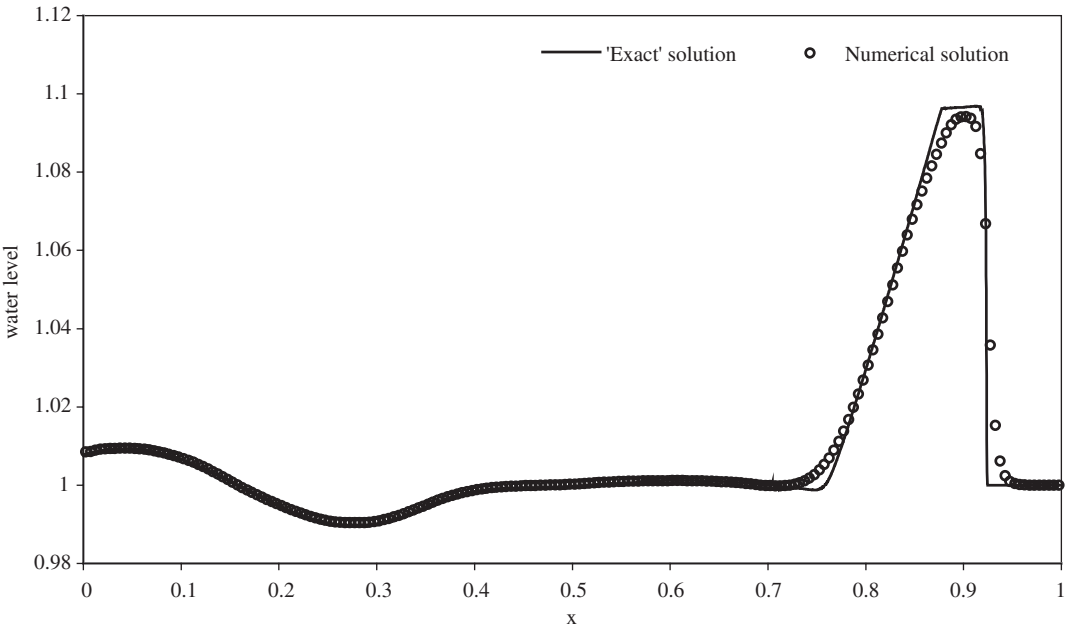

Figure 18. LeVeque test example with $\varepsilon = 0.2$. Comparison of water level at $t = 0.7$ s, Section 4.2.6.

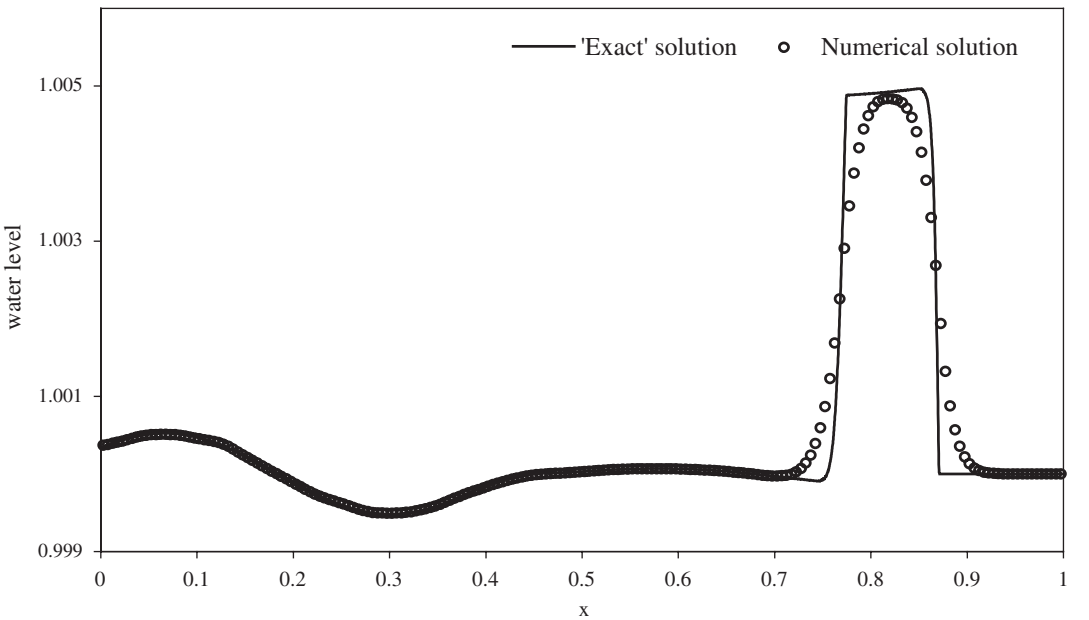

Figure 19. LeVeque test example with $\varepsilon = 0.01$. Comparison of water level at $t = 0.7$ s, Section 4.2.6.

is obtained with the third order balanced WENO-LLF scheme [15] on a fine grid with 10 000 cells. This scheme is used because we know it is high resolution and high order accurate. We can see that the balanced central NT scheme captures the quasi-steady state very well.

4.2.7. Two test problems for transcritical flow over a bump. We consider here two cases: in the first a smooth transition occurs while in the second a hydraulic jump arises. The bump is defined with

$$z(x) = \begin{cases} 0.2 - 0.05(x-10)^2 & \text{if } 8 < x < 12 \\ 0 & \text{otherwise} \end{cases} \tag{49}$$

The computational domain is 25 m long. Depending on the boundary conditions we set, the flow becomes supercritical and then it reverses or not to the subcritical.

For the case of the steady transcritical flow with a smooth transition, a discharge of $1.53\ \mathrm{m}^2/\mathrm{s}$ is imposed on the upstream boundary. With the given discharge the flow becomes supercritical over the bump and it remain supercritical downstream of the bump, therefore the downstream boundary condition is not needed in that case.

To obtain a hydraulic jump, on the upstream boundary the discharge is set to $0.18\ \mathrm{m}^2/\mathrm{s}$, while on the downstream boundary a constant water elevation $h(25, t) = 0.33$ m is imposed.

The numerical parameters in both the cases are $\Delta x = 0.125$, and $c_{\mathrm{cfl}} = 0.5$. The results are presented in Figures 20 and 21 for the smooth transition case and in Figures 22 and 23 for the hydraulic jump case. We can notice that the numerically evaluated water level coincides quite well with the analytical solution in both cases. The numerical instabilities occur in

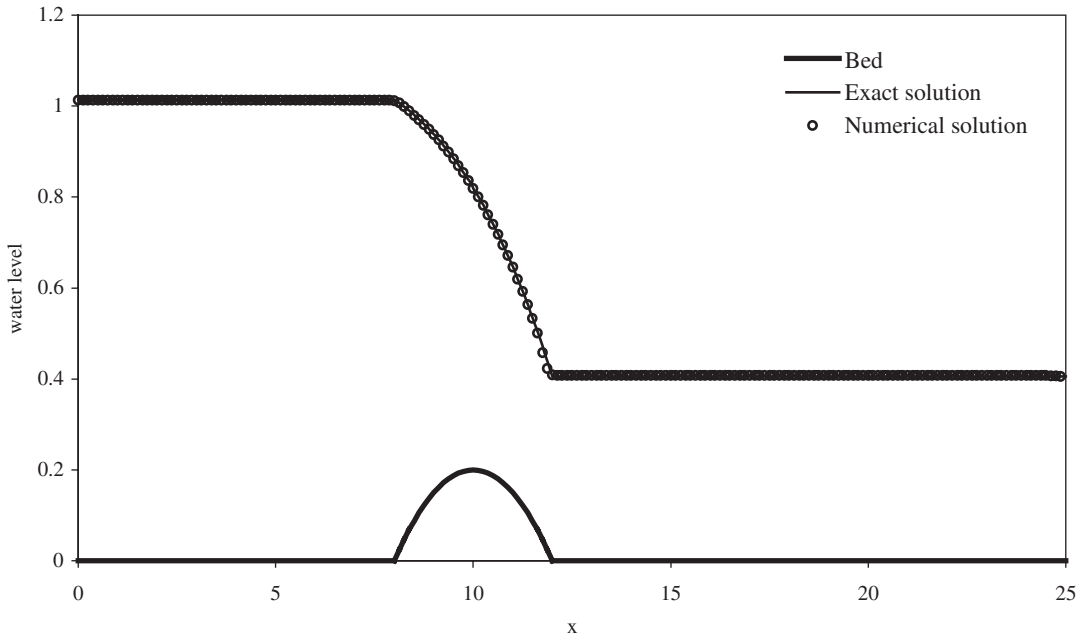

Figure 20. Water level for the test with a smooth transition, Section 4.2.7.

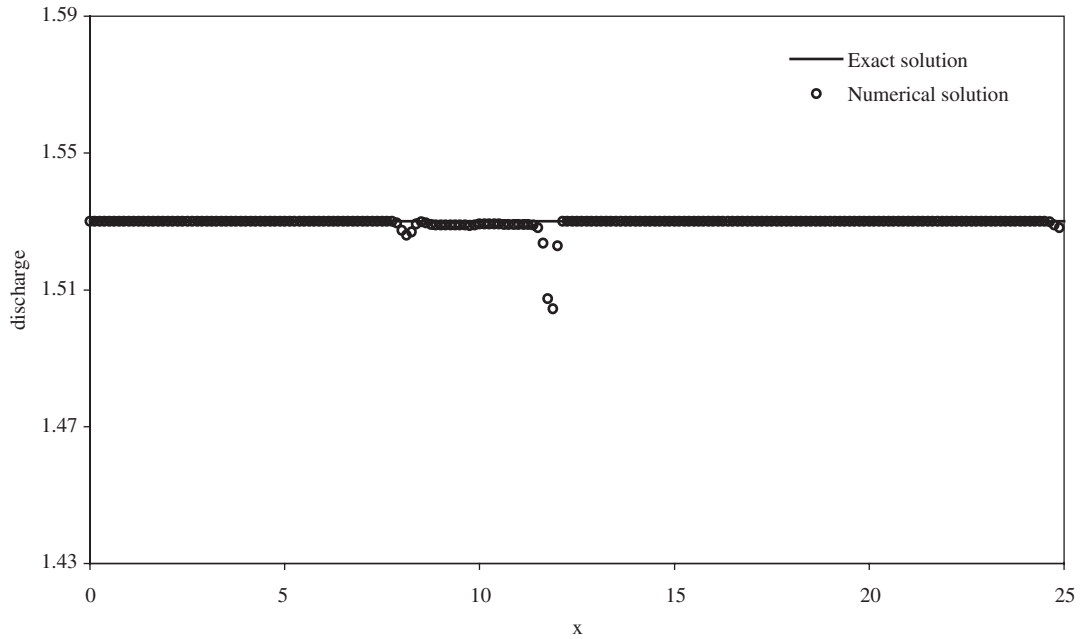

Figure 21. Discharge for the test with a smooth transition, Section 4.2.7.

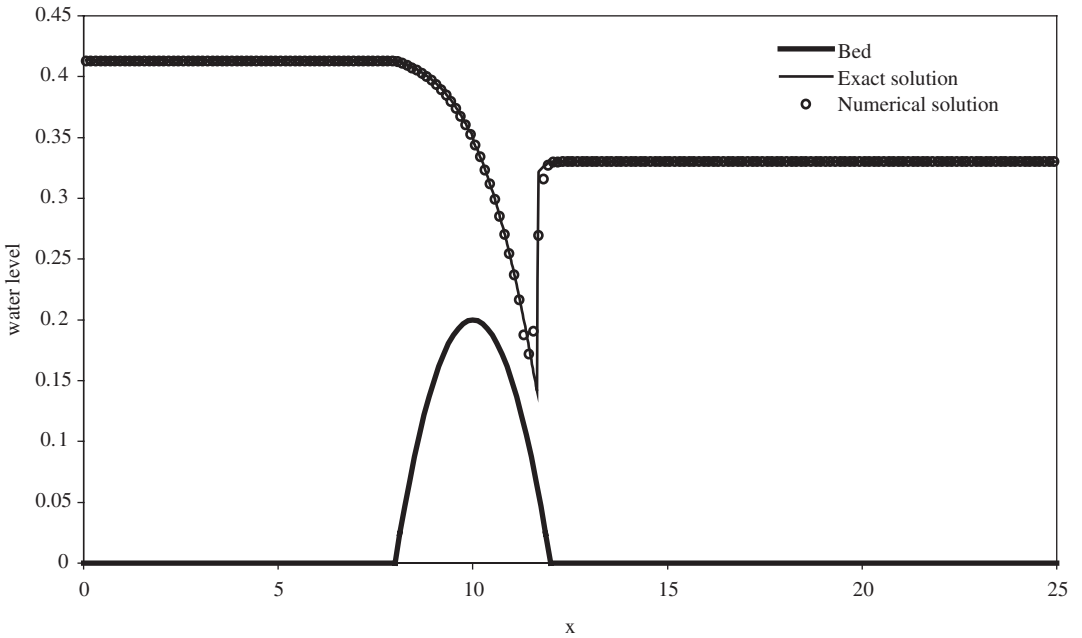

Figure 22. Water level for the test with a hydraulic jump, Section 4.2.7.

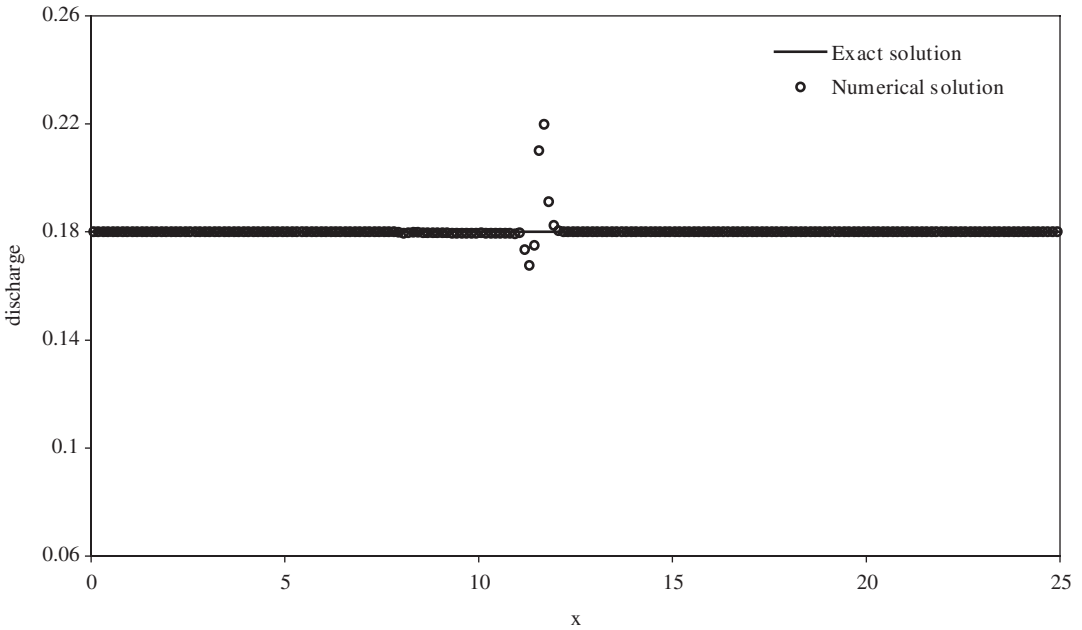

Figure 23. Discharge for the test with a hydraulic jump, Section 4.2.7.

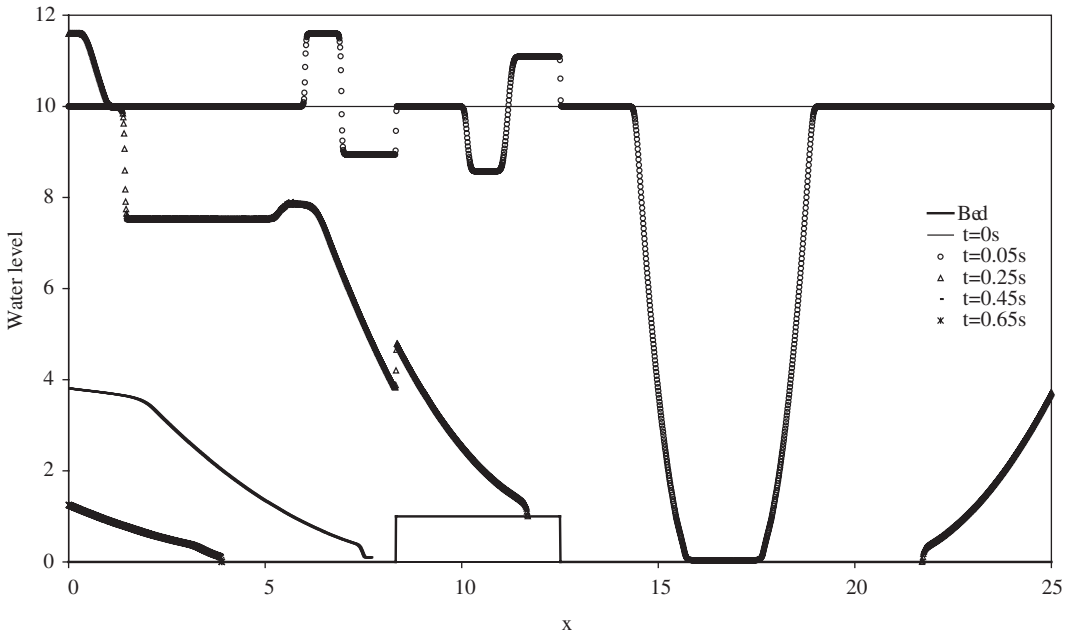

Figure 24. Water level evolution for the rarefaction waves over a step, Section 4.2.8.

the numerical discharge over the place where the riverbed bump joins with the flat bottom. The similar phenomenon can be noticed in Reference [8] where the surface gradient method combined with the MUSCL finite volume type scheme is used. Hence we think that the presented numerical errors are the consequence of the linear interpolation procedure used. Larger numerical errors in the discharge occur at the hydraulic jump. Such a numerical error at the jump is common for all the known numerical schemes.

4.2.8. Rarefaction over a rectangular bump. This is a test that consists of the two rarefaction waves, but with an addition of a nontrivial topography. This test problem was proposed in Reference [15], where it was used to test the behaviour of the numerical scheme over dry bed. The bottom topography is defined with

$$z(x)=\begin{cases}1 & \text{if } 25/3<x<12.5\\ 0 & \text{otherwise}\end{cases} \tag{50}$$

The initial water level height is 10 m, while the initial discharge is

$$Q(x,0)=\begin{cases}-350 & \text{if } x<50/3\\ 350 & \text{otherwise}\end{cases} \tag{51}$$

We do not analyse here the influence of the dry cells, but we use this test just to illustrate good behaviour of our schemes in a more complicated water flow situations. The numerical water level profiles at different times are presented in Figure 24. When we compare the obtained

results with the results presented in Reference [16] we can conclude they coincide very well. Although the central NT scheme works well on this test example, this is not general for all the cases where a dry riverbed appears. The numerical treatment of the dry bed needs an additional attention and requires further study.

5. CONCLUSIONS

In this paper we presented the extension of the non-staggered central NT schemes to the balance laws with the geometrical source terms. The crucial property we want to achieve with this numerical scheme is to preserve some steady state solutions. In order to do this we must consider a particular balance law. Here the complete definition of the balanced scheme is presented for the Burger's equation and for the shallow-water system. In both cases the obtained numerical scheme gives very good results in steady and unsteady flow cases. The additional extension of the central NT scheme could be connected with numerical handling of the spatially varied flux in hyperbolic laws, just as the upwind and high resolution schemes were extended in the one-dimensional open-channel flow case [17, 18]. Further work could be related to the extension of the considered numerical scheme to the one-dimensional sediment transport equations by following the numerical approach used in Reference [19].

REFERENCES

1. LeVeque RJ. *Finite Volume Methods for Hyperbolic Problems*. Cambridge University Press: Cambridge, 2002.
2. Jin S. A steady-state capturing method for hyperbolic systems with geometrical source terms. *Mathematical Modelling and Numerical Analysis* 2001; **35**:631–646.
3. Jin S, Levermore CD. Numerical schemes for hyperbolic conservation laws with stiff relaxation terms. *Journal of Computational Physics* 1996; **126**:449–467.
4. Bermùdez A, Vázquez ME. Upwind methods for hyperbolic conservation laws with source terms. *Computers and Fluids* 1994; **23**(8):1049–1071.
5. Vázquez-Cendón ME. Improved treatment of source terms in upwind schemes for the shallow water equations in channel with irregular geometry. *Journal of Computational Physics* 1999; **148**:497–526.
6. Hubbard ME, García-Navarro P. Flux difference splitting and the balancing of source terms and flux gradient. *Journal of Computational Physics* 2000; **165**:89–112.
7. LeVeque RJ. Balancing source terms and flux gradients in high-resolution Godunov methods: the quasi-steady wave propagation algorithm. *Journal of Computational Physics* 1998; **146**:346–365.
8. Zhou JG, Causon DM, Mingham CG, Ingram DM. The surface gradient method for the treatment of source terms in the shallow-water equations. *Journal of Computational Physics* 2001; **168**:1–25.
9. Xu K. A well-balanced gas-kinetic scheme for the shallow-water equations with source terms. *Journal of Computational Physics* 2000; **178**:533–562.
10. Kurganov A, Levy D. Central-upwind schemes for the Saint-Venant system. *Mathematical Modelling and Numerical Analysis* 1999; **33**(3):547–571.
11. Rogers BD, Borthwick AGL, Taylor PH. Mathematical balancing of flux gradient and source terms prior to using Roe's approximate Riemann solver. *Journal of Computational Physics* 2003; **192**:422–451.
12. Jiang G-S, Levy D, Lin C-T, Osher S, Tadmor E. High-resolution nonoscillatory central schemes with nonstaggered grids for hyperbolic conservation laws. *SIAM Journal on Numerical Analysis* 1998; **35**(6): 2147–2168.
13. Liotta SF, Romano V, Russo G. Central schemes for balance laws of relaxation type. *SIAM Journal on Numerical Analysis* 2000; **38**(4):1337–1356.
14. Zhou JG, Causon DM, Ingram DM, Mingham CG. Numerical solutions of the shallow water equations with discontinuous bed topography. *International Journal for Numerical Methods in Fluids* 2002; **38**:769–788.
15. Vuković S, Sopta L. ENO and WENO schemes with the exact conservation property for one-dimensional shallow water equations. *Journal of Computational Physics* 2002; **179**:593–621.
16. Gallouët T, Hérard J-M, Seguin N. Some approximate Godunov schemes to compute shallow water equations with topography. *Computers and Fluids* 2003; **32**:479–513.

17. Vuković S, Sopta L. Upwind schemes with exact conservation property for one-dimensional open channel flow equations. *SIAM Journal on Science and Computing* 2003; **24**(5):1630–1649.
18. Vuković S, Črnjarić-Žic N, Sopta L. ENO and WENO schemes for balance laws with spatially varying flux functions. *Journal of Computational Physics* 2004, in press.
19. Črnjarić-Žic N, Vuković S, Sopta L. Extension of ENO and WENO schemes to one-dimensional sediment transport equations. *Computers and Fluids* 2003; **33**(1):31–56.

